Conformational Dependence of Intramolecular Vibrational Energy Redistribution in the Ethylenic=CH_2 Stretch Fundamental of Allyl Fluoride

David A. McWhorter and Brooks H. Pate*

Department of Chemistry, University of Virginia, Charlottesville, Virginia 22901

Received: June 12, 1998; In Final Form: August 24, 1998

The high-resolution (6 MHz) infrared spectra of the asymmetric ethylenic hydride stretches of both cis and gauche allyl fluoride have been measured. Rotational assignments of the eigenstates are made using the ground-state microwave-infrared double-resonance capabilities of an electric resonance optothermal spectrometer (EROS). The cis vibrational band near 3114 cm^{-1} is characterized by sparse, narrow IVR multiplets resulting from weak Coriolis or cross conformer interactions between the vibrational bath states. The IVR lifetime of the cis vibrational band is approximately 2 ns (2000 ps). The gauche vibrational band near 3100 cm^{-1} is qualitatively and quantitatively quite different from the cis band. The gauche band is characterized by significantly fragmented IVR multiplets with an average IVR lifetime of about 90 ps. The measured anharmonic state density of the gauche band is about 30 states/cm^{-1}. The disagreement between the measured state densities of the gauche vibrational band and the calculated values suggest that the gauche vibrational states do not interact with cis vibrational states. For two IVR multiplets of the gauche band, the transitions were assigned according to the parity of the rovibrational bright state. The two parity states show roughly the same dynamical behavior. Also, RRKM calculations of the unimolecular isomerization rate are performed and compared to experimental results. The RRKM calculations overestimate both the cis and gauche isomerization rates by orders of magnitude.

Introduction

Vibrational energy flow in polyatomic molecules plays a fundamental role in chemical kinetics.[1−3] Statistical theories of reaction rates, such as RRKM theory, assume that intramolecular vibrational energy redistribution (IVR) is complete on a time scale much faster than the rate of reaction.[1,4] In the past decade, measurements of the initial rate of energy redistribution using both time-domain[2,5] and frequency-domain[6−8] techniques have been made to test this underlying assumption. In particular, high-resolution spectroscopy is capable of testing both aspects of this premise. The high-resolution spectrum provides a quantitative measure of the initial IVR rate of the optically active vibrational mode (often called the bright state) through the line shape profile of the spectrum.[2,3] The issue of whether all energetically accessible quantum states participate in the dynamics can be addressed through comparisons of measured and calculated state densities.

High-resolution spectroscopic studies of IVR in the hydride stretch fundamentals and low overtones of polyatomic molecules have found that the time scale for energy localization ranges from tens of picoseconds to a few nanoseconds.[2] The complete set of experimental IVR rate determinations has suggested a chemical nature for the IVR rate. For example, it is generally found that acetylenic C−H stretches show slower initial IVR rates than other hydride stretches. Also, the O−H stretches tend to have the fastest rates. These results have led to several proposed structure correlations for IVR rates that focus on the type of hydride stretch[2,9] (e.g., O−H vs ≡C−H stretches) or on the proximity of the vibrational mode to large amplitude coordinates.[10,11] Although general trends have been observed, one problem is that the distribution of measured IVR rates leads to several counterexamples for the general correlations.

One possibility for determining the typical distribution for measured IVR rates that might be caused by fluctuations in the identity of the near-resonant vibrational bath, may be found by comparing the IVR rates for the same normal-mode vibration in different conformers of the same molecule. The rapid cooling present in the free jet expansion often leads to large populations of two or more conformers.[12] The vibrational spectra of both forms can then be investigated to provide two independent spectra where the intramolecular vibrational couplings are expected to be similar. The previous investigation of the acetylenic C−H stretch of 1-pentyne determined that the IVR rates of the two conformers differ by about a factor of 2.[13] Here, we present a high-resolution infrared spectroscopy study of the ethylenic=CH_2 stretch of two conformers of allyl fluoride (3-fluoropropene: $H_2C{=}CHCH_2F$). In this case, we find dramatic differences in the IVR dynamics that we attribute to restricted interactions between vibrational states associated with the two different conformers.

The study of the high-resolution spectra of different conformers can also provide information about the unimolecular conformational isomerization reaction at a well-defined total energy of the molecule.[14−17] Conformational isomerization about single bonds plays a key role in the reactivity of small molecules, for example, the Diels−Alder reaction, and is fundamental to the structure and function of large molecules of biological interest. Unimolecular reaction studies generally show excellent agreement with RRKM predictions.[1,18] However, the case of unimolecular isomerization about low barriers appears to be a class of unimolecular reactions that are very poorly described by the statistical theory.[19−21] We have recently measured the isomerization rate of 2-fluoroethanol at 2980 cm^{-1} and find that the rate is about 3 orders-of-magnitude slower than predicted.[15,16]

10.1021/jp982609g CCC: $15.00
Published on Web 10/10/1998

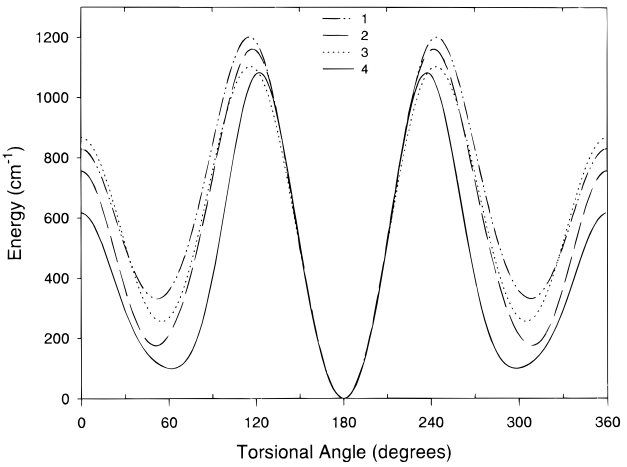

Figure 1. Shown here are four torsional potentials for allyl fluoride as reported from experimental and ab initio studies. Curve 1 is from the infrared study of ref 29, curve 2 is from the ab initio computations of the current study (HF/6-311G**), curve 3 is reported from ab initio calculations of ref 31 (MP2/6-31G**), and curve 4 is the result of the microwave and far-infrared work of ref 28.

For this class of reactions, the intramolecular dynamics may be sufficiently slow that the fundamental assumption of rapid and complete IVR is invalid, leading to a case that has been called "IVR-limited" reactions.[19−21] In this and the following paper[22] we demonstrate how high-resolution spectroscopy can be used to investigate the origin of the slow isomerization rates.

Experimental Section

The sample of allyl fluoride (3-fluoropropene, C_3H_5F) was obtained from PCR, Inc. The pure sample is diluted in He to approximately 3% and the gas mixture is then expanded through a 50 μm pinhole nozzle to form the molecular beam.

A detailed description of the electric resonance optothermal spectrometer (EROS) and its double resonance mechanism has been reported previously.[23,24] The original design of Fraser and Pine[25] has been modified to extend the microwave-infrared double resonance capabilities of the spectrometer. Briefly, a color center laser, pumped by a Kr^+ laser, provides about 12 mW of tunable cw infrared radiation in the 3095−3120 cm^{-1} frequency range. The laser output makes approximately 14 crosses with the molecular-beam as it passes through a gold-plated mirror, plane-parallel multipass assembly. The microwave coupling assembly is placed under the laser multipass such that the infrared and microwave irradiation areas overlap in space. The available microwave frequency is 100 kHz−62 GHz with approximately 30 mW (15 dBm) of power across the full range. All infrared rotational assignments are made using ground-state microwave-infrared double resonance to ensure that all transitions originate from the ground torsional states of either the cis or gauche conformer.[24] Upon exiting the source chamber, the molecular-beam passes through a 1 mm conical skimmer and into the state-focusing assembly. The detector is a composite silicon bolometer cooled to 1.5 K.

Torsional Potential for Allyl Fluoride. Internal rotation about the C−C single bond in allyl fluoride gives rise to two stable conformers.[26,27] Spectroscopic studies in the microwave and far-infrared spectral regions have been used to determine the potential curve for this motion.[28−30] The two experimentally derived potentials[28,29] and potentials calculated by ab initio methods[31] are shown in Figure 1. In general, there is good agreement between the experimental and ab initio results.[32] The

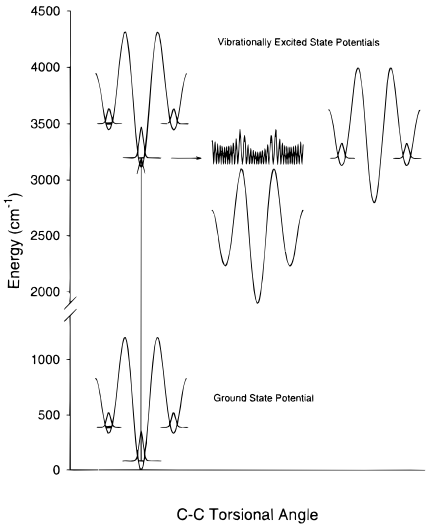

Figure 2. An adiabatic depiction of vibrational state mixing is shown. Here, each normal-mode vibrational state has its own C−C torsional potential energy curve. The infrared spectra originate in the lowest torsional level of the ground-state potential of either the cis or gauche conformer wells. The probabilities of the $v = 0$ wave functions for the cis and gauche states are given for the ground-state potential. The infrared transition occurs to the lowest torsional level of the asymmetric ethylenic hydride stretch near 3114 and 3100 cm^{-1} for the cis and gauche conformers, respectively. This transition is indicated by the vertical arrow for the case of excitation of the cis conformer. In the energy region of the cis $=CH_2$ bright state, there are other states that have torsional wave functions either localized about the cis conformation (not shown), delocalized over the isomerization barrier (middle potential), or localized about the gauche conformation (seen on the right). The conformational isomerization process involves coupling between states with different torsional character (e.g., cis and gauche).

more stable form of the molecule is the cis conformation. The gauche conformer is less stable by approximately 300 cm^{-1}. There are two equivalent gauche structures that correspond to the enantiomers of this structure. The barrier to conversion between the two gauche enantiomers is approximately 450 cm^{-1}, and the barrier to conformational isomerization between the ground cis torsional state and the ground gauche state is 1100 cm^{-1}.

We discuss the vibrational spectroscopy of allyl fluoride using a model that separates the large amplitude torsional motion from the other normal-mode vibrations.[14] For example, we can define a torsional potential for the molecule with the asymmetric $=CH_2$ hydride stretch normal-mode vibration excited. Physically, it is reasonable to assume that the torsional potential is relatively unchanged when this normal mode vibration is excited. This idea is illustrated in Figure 2. In the molecular beam we populate both the ground cis and gauche torsional states. The infrared transition for the asymmetric $=CH_2$ stretch vibration, near 3100 cm^{-1}, does not change the torsional quantum numbers so that the spectroscopy resembles the model used for electronic spectroscopy. In this case, the torsional wave functions provide the "Franck−Condon" factors. Because the potentials in the ground and $=CH_2$ stretch state are expected to be similar, the only transitions that will be observed are those between the ground torsional states. Experimentally, these transitions are observed at 3114 cm^{-1} for the cis conformer and 3100 cm^{-1} for the gauche.[30] The final state for the gauche vibrational transition lies approximately 290 cm^{-1} higher in absolute energy than the cis final state due to the energy difference between the conformers. In terms of the model we have adopted, the

frequency difference is attributed to a 14 cm^{-1} (4.8%) relative stabilization of the gauche conformer in the excited state.

The vibrational spectroscopy of the cis conformer is straightforward because this conformer corresponds to a single well in the torsional potential. For the gauche conformer, there are two nearly degenerate "ground" states arising from the symmetric and antisymmetric combinations of the $v = 0$ states of each of the double wells.[28] The tunneling splitting of these states has been measured by microwave spectroscopy and is 125 ± 15 kHz.[28] In the molecular beam, both of these states have equal population. Therefore, the vibrational spectrum of the gauche conformer contains two overlapping spectra. Because the tunneling splitting is resolvable in the microwave spectrum, it is possible in some cases to separately assign these spectra using ground-state microwave-infrared double-resonance spectroscopy.

In the energy region of the asymmetric $=CH_2$ stretch, there will be many other vibrational quantum states that are overtones and combination bands of the other lower frequency normal-mode vibrations.[2,3] To describe these near-resonant states we can also adiabatically separate the torsional motion from the other normal-mode vibrations. Each normal-mode combination or overtone state is assigned a C−C torsional potential. Within this model we can assign the near-resonant vibrational states at 3100 cm^{-1} on the basis of the character of their torsional wave function. Some of the nearby states will have torsional wave functions that are localized around the cis or gauche conformations. Others will have torsional wave functions that are above the barrier to isomerization and are, therefore, delocalized in the torsional coordinate. These types of near-resonant states are illustrated in Figure 2.

These vibrational states will interact through higher order terms in the Hamiltonian giving rise to IVR. In the high-resolution infrared spectrum, the flow of vibrational energy between these states is manifested by extensive local perturbations in the spectrum giving rise to a "multiplet" structure for each rovibrational transition.[2,3] Using this separation, the conformational isomerization process is viewed as the coupling between states with different torsional character (i.e., cis and gauche) through anharmonic or rotationally mediated interactions (e.g., Coriolis or centrifugal coupling mechanisms). The interaction between these different types of states may require the participation of a delocalized torsional state, or isomerization state.[14,16,33]

IVR Dynamics of the cis and gauche Conformers. The high-resolution infrared spectra of the cis and gauche conformers of allyl fluoride are qualitatively different as seen in Figure 3. The spectrum of the cis conformer is relatively unperturbed and exhibits only weak interactions with the near-resonant vibrational states. The IVR rate for this conformer is exceptionally slow (<1 ns^{-1}). In contrast, the spectrum of the gauche conformer is extensively fragmented through vibrational coupling to the near-resonant states and has an IVR rate at least an order-of-magnitude faster than found for the cis conformer (90 ps^{-1}). These results are presented below along with an analysis of the types of near-resonant states (i.e., cis, gauche, or delocalized) for the cis and gauche spectra. From this analysis we propose that the differences between these two spectra indicate that conformational isomerization occurs on a much slower time scale than IVR between vibrational states of a single conformer.[16,17]

IVR of the Cis Conformer. We have assigned 25 IVR multiplets of the asymmetric $=CH_2$ stretch, near 3114 cm^{-1}, using ground-state microwave-infrared double-resonance spectroscopy.[34] This vibrational band is predominantly an a-type

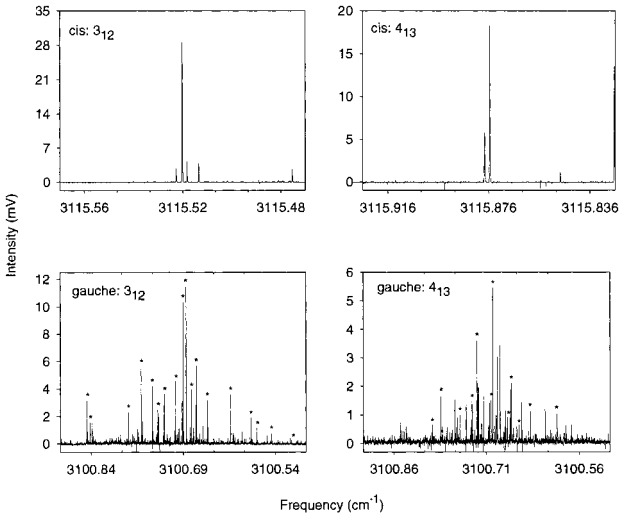

Figure 3. A comparison of IVR multiplets in the cis and gauche vibrational bands is shown. The top panels are representative examples of the IVR multiplet structure observed in the cis band. The 3_{12} and 4_{13} multiplets are narrow and sparse, containing only 4 and 2 eigenstates, respectively. In contrast, the gauche multiplets are much more fragmented and span a larger frequency area (note the frequency scale here is four times the top frames). Several of the eigenstates in the 3_{12} and 4_{13} multiplets are marked with asterisks in the bottom panels. The total number of eigenstates assigned to these multiplets is 56 and 40, respectively.

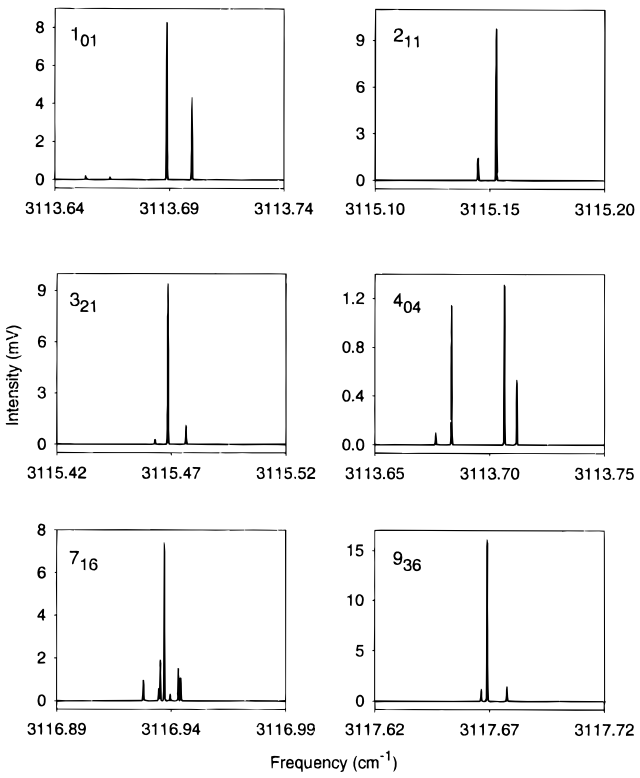

Figure 4. Shown here are reproduced (noiseless) spectra of several cis IVR multiplets. Even over the large range of J and K_a seen here, the IVR multiplets remain narrow and sparse. The 4_{04} multiplet is the broadest of all the cis multiplets with the next broadest being the 1_{01}. Typical IVR lifetimes for these multiplets are calculated on the order of 2 ns.

band. The assigned multiplets range from $J = 0-9$ and $K_a = 0-3$. A sample of these multiplets is shown in Figure 4. In general, the multiplets are narrow and show only a few closely spaced transitions. We have calculated the time scale for IVR

TABLE 1: Spectroscopic and IVR Data for the Asymmetric Ethylenic Stretch Vibrational Band of cis-Allyl Fluoride

IR transition ($J'_{K_a'K_c'}$-$J''_{K_a''K_c''}$)	center frequency (cm^{-1})	no. of eigenstates	state density (states/cm^{-1})
$0_{00}-1_{01}$	3114.03	2	63
$1_{01}-2_{02}$	3113.69	4	65
$1_{11}-2_{12}$	3113.72	2	109
$1_{10}-2_{11}$	3113.64	3	175
$2_{02}-1_{01}$	3115.11	1	
$2_{12}-3_{13}$	3113.41	2	409
$2_{11}-3_{12}$	3115.15	2	126
$2_{21}-3_{22}$	3113.33	2	295
$2_{20}-3_{21}$	3113.32	6	415
$3_{03}-2_{02}$	3115.43	2	516
$3_{12}-2_{11}$	3115.51	4	330
$3_{22}-2_{21}$	3115.45	5	90
$3_{21}-2_{20}$	3115.47	3	148
$4_{04}-4_{13}$	3113.70	4	85
$4_{13}-3_{12}$	3115.88	2	500
$4_{23}-3_{22}$	3115.80	7	137
$4_{22}-3_{21}$	3115.84	5	58
$6_{16}-5_{15}$	3116.41	3	102
$6_{25}-5_{24}$	3116.33	5	125
$7_{16}-6_{15}$	3116.94	7	369
$7_{25}-6_{24}$	3116.98	3	80
$8_{17}-7_{16}$	3117.28	3	319
$8_{26}-7_{25}$	3117.37	3	264
$9_{27}-8_{25}$	3117.75	4	97
$9_{36}-8_{35}$	3117.66	3	179

through the survival probability[35]

$$P(t) = |\langle\Psi(0)|\Psi(t)\rangle|^2 \quad (1)$$

where $\Psi(0)$ is a single rotational level of the asymmetric =CH_2 stretch of the cis conformer. Because the number of transitions in the individual multiplets is small, this quantity does not show smooth decay but instead displays strong recurrence or "ringing" behavior in many cases. In Table 1 we report the quantities related to the IVR process. Because the IVR multiplets are so sparse, it is difficult to determine a decay time for the survival probability for the majority of the multiplets. However, using only the IVR multiplets that contain 5 or more eigenstates, such that a decay time can be approximated, an estimate of 2 ns for the IVR lifetime is obtained. We have also investigated the $P(t)$ of all the IVR multiplets (except 2_{02}) with respect to the average $P(t)$ at long times, given by $(N_{eff})^{-1}$ (or the dilution factor).[36] This analysis results in an average τ_{IVR} of approximately 1.6 ns.

IVR of the Gauche Conformer. The asymmetric =CH_2 stretch of the gauche conformer is an a−b hybrid band with a band origin near 3100 cm^{-1}. We have assigned 10 rotational levels of this spectrum[34] and some of the IVR multiplets are shown in Figure 5. This band has a qualitatively different appearance from the cis spectra. The individual multiplets are considerably broader, reflecting a much faster IVR rate, and contain many more eigenstates. The IVR lifetimes for each rotational level, determined from the survival probability, are given in Table 2 along with other IVR quantities. For the calculation of the state density, we have considered only the central portions of the multiplets. For the 3_{12} and 4_{13} IVR multiplets, we have taken the central 20 lines and for the remaining multiplets we have used the central 10 lines for the calculation of the state density. In this way, we avoid the wings of the multiplet where lower sensitivity may artificially reduce the value calculated for the state density.[37] In Table 2 we have used all transitions appearing in the multiplet even though there are actually two overlapped spectra present, as discussed above.

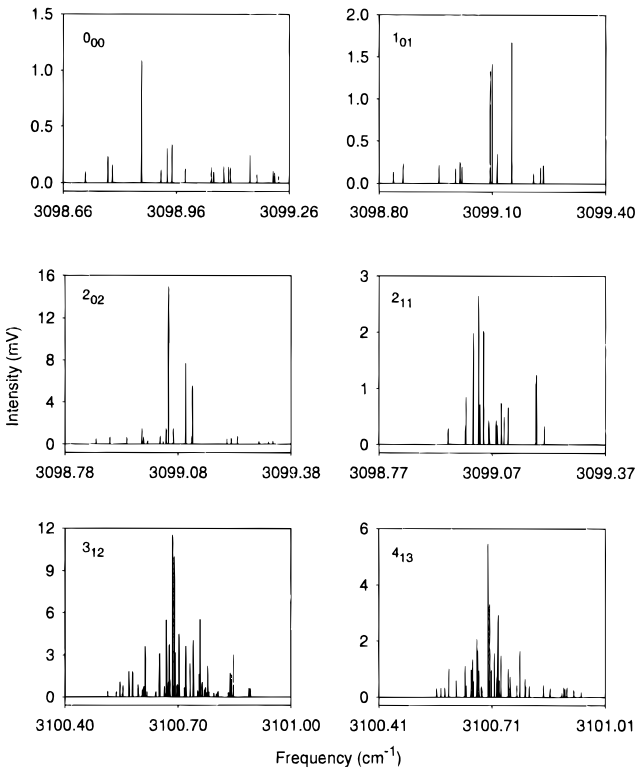

Figure 5. Several reproduced (noiseless) spectra of the gauche vibrational band are shown. All of these multiplets are actually two overlapping spectra that result from the nearly degenerate symmetric and antisymmetric combinations of the $v = 0$ states of each gauche torsional potential well.

TABLE 2: Spectroscopic and IVR Data for the Asymmetric Ethylenic Stretch Vibrational Band of gauche-Allyl Fluoride

IR transition ($J'_{K_a'K_c'}$-$J''_{K_a''K_c''}$)	center frequency (cm^{-1})	no. of eigenstates	τ_{IVR} (ps)	state density (states/cm^{-1})
$0_{00}-1_{11}$	3098.96	18	32.62	29
$1_{01}-2_{10}$	3099.10	13	65.65	33
$2_{02}-3_{03}$	3099.08	21	81.54	75
$2_{12}-3_{13}$	3099.08	15	83.03	76
$2_{11}-3_{12}$	3099.06	16	90.65	115
$3_{03}-3_{12}$	3099.12	8	111.04	36
$3_{13}-2_{02}$	3101.51	12	106.94	47
$3_{12}-3_{03}$	3100.70	56	71.09	217
$4_{14}-3_{03}$	3101.78	15	118.94	102
$4_{13}-4_{04}$	3100.71	40	79.02	151

The IVR lifetimes are found to be rotationally independent as shown in Figure 6. The one exception is that the lifetime for the rotationless 0_{00} level is about a factor of 2 shorter. A similar effect has been observed in the dynamics of the O−H stretch fundamental of propynol[38] and in the O−H stretch overtones of methanol.[39] This effect is likely related to the finite signal-to-noise of our experiment. The spectral state density clearly increases with total angular momentum J, as seen in Figure 5. As the state density increases, the intensity of transitions in the wings of the spectrum decreases and can drop below the signal-to-noise threshold. Missing transitions in the wings leads to an overestimate of the IVR lifetime. The average IVR lifetime (excluding the 0_{00} state) is 90 ps. This lifetime is similar to other measured hydride stretch lifetimes[2,10] and, in particular, is similar to the lifetime of the asymmetric =CH_2 stretch of isobutene (H_2C=$C(CH_3)_2$).[37]

For the 3_{12} and 4_{13} IVR multiplets we have been able to separate the two independent spectra for the gauche conformer.

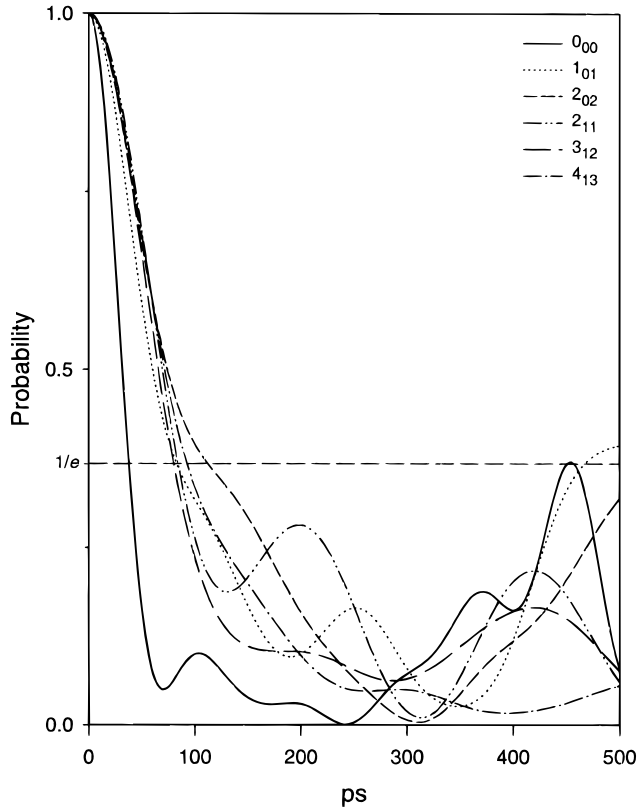

Figure 6. The survival probabilities of the gauche IVR multiplets are shown. With the exception of the 0_{00} IVR multiplet, the initial decays of the survival probabilities are largely independent of the total angular momentum *J*.

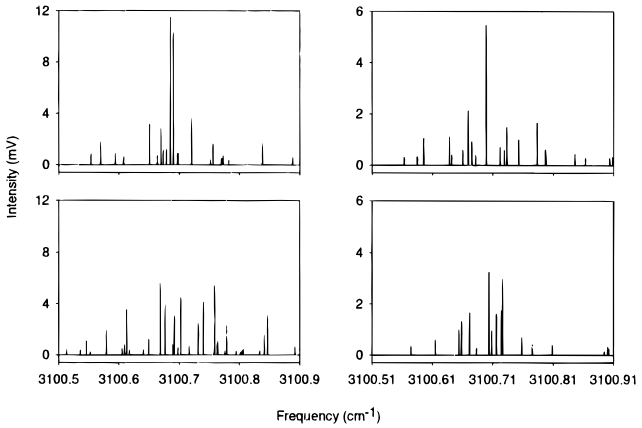

Figure 7. The two overlapping spectra that originate from the nearly degenerate symmetric and antisymmetric combinations of the $v = 0$ states of each gauche torsional potential well, have been separated through ground-state microwave-infrared double resonance. The 3_{12} spectra are shown on the left and the 4_{13} are on the right. Some of the spectral properties of the separated multiplets shown here, are given in Table 3. The top panels of the figure show the transitions of the "full" multiplets that are in double-resonance with the lower frequency component of the c-type microwave transition used for assignment.

The c-type pure rotational transitions occur between rotational levels of the symmetric (+) and antisymmetric (−) torsional tunneling states.[28] For allyl fluoride the tunneling splitting is large enough (125 ± 15 MHz) for us to resolve the two different c-type transitions (i.e., the $3_{12}(+)-3_{03}(-)$ and the $3_{12}(-)-3_{03}(+)$ are split by twice the tunneling splitting). The separate IVR multiplets are shown in Figure 7. The IVR lifetimes, center frequencies, total intensities, and state densities of the separate spectra are given in Table 3. As expected, the centers-of-gravityand total intensities of each multiplet are identical within experimental uncertainties. This result reflects the fact that the tunneling splitting is largely unchanged in the asymmetric $=CH_2$ stretch normal-mode vibrational state of the gauche conformer. Despite the qualitatively different line shape profiles of the separate spectra, the IVR lifetimes of the two states are similar and within the fluctuations found in the lifetime determinations over all multiplets.

The Nature of the Near-Resonant Vibrational States. Using the model where the torsional motion is adiabatically separated from the normal-mode vibrations, we can determine the local density of cis, gauche, and delocalized torsional states using direct state-count methods.[40,41] In this calculation, we use the normal-mode frequencies that have been previously assigned.[30] All normal-mode vibrational states are assumed to have the same torsional potential and the torsional states are calculated by diagonalizing the one-dimensional hindered rotation Hamiltonian using a free-rotor basis set.[42] The torsional characterization of the vibrational states in the energy regions of the cis and gauche asymmetric $=CH_2$ stretch normal-mode vibrational states (3114 and 3410 cm^{-1} with respect to the ground vibrational state (cis)) are given in Table 4. When considering the IVR dynamics of a given bright-state with no rotation (i.e., the 0_{00} rotational state of the asymmetric rotor), intramolecular interactions can occur only for states that have the same vibrational symmetry as the bright state. The values of state density given in Table 4 are the full density of states of both symmetries (A′ and A″ of the planar C_s point group); however, a single-symmetry bright state only interacts with half of these states. For higher rotational levels, parity restrictions still permit coupling to only half of the total states through anharmonic and rotationally mediated (e.g., Coriolis and centrifugal) interactions. In the experimental spectra of the gauche conformer, both symmetry species (parities) of the bright state are present (i.e., there are two overlapped spectra) and thus we expect to see the full state density (given in Table 4) in the infrared spectra.

For the cis conformer, the full density of vibrational states of the same symmetry as the $=CH_2$ stretch bright state is approximately 10 states/cm^{-1}. For polyatomic molecules, there is critical state density required to observe extensive IVR. High-resolution infrared spectroscopy studies of other molecules (≡C−H hydride stretch of propynol:[38] 19 states/cm^{-1}, $-CH_3$ hydride stretch of 1-butyne,[36] 9 (A symmetry) and 18 (E symmetry) states/cm^{-1}, and propargylamine,[43] 16 states/cm^{-1}) suggest that this full state density of proper symmetry is sufficient to observe extensive IVR. On the basis of the studies of other hydride stretches, an IVR lifetime of 10−500 ps might be expected.[2,10] Instead, we observe very slow IVR with little fragmentation.

For the gauche conformer, with a total state density of about 17 states/cm^{-1} of the same symmetry as the bright-state, a "typical" hydride stretch spectrum is observed. We attribute the different dynamics of these two conformers to the local density of vibrational states of the same conformation. For the cis conformer, the state density for other *cis*-like states of proper symmetry is only 3.5 states/cm^{-1} and is well below the threshold for observing extensive IVR.[44,45] However, for the gauche conformer, the density of gauche-like states of proper symmetry is 8.5 states/cm^{-1} placing near the critical state-density threshold.[44,45] If the coupling between vibrational states of the same conformation is significantly stronger than the coupling between states of different conformation, then these conformers would be expected to show different behavior.

TABLE 3: Spectroscopic and IVR Data for the Separated 3_{12} and 4_{13} Multiplets of gauche-Allyl Fluoride

IR transition ($J'_{K_a'K_c'}$-$J''_{K_a''K_c''}$)	center frequency (cm^{-1})	double−resonance frequency−transition (MHz-$J'_{K_a'K_c'}$-$J''_{K_a''K_c''}$)	total intensity (mV)	no. of eigenstates	τ_{IVR} (ps)	state density (states/cm^{-1})
$3_{12}-3_{03}$	3100.69095	23 130.700−($3_{13}-3_{03}$)	48.02	23	99.93	109
$3_{12}-3_{03}$	3100.70885	23 130.955−($3_{13}-3_{03}$)	53.76	33	61.73	104
$4_{13}-4_{04}$	3101.71230	22 872.365−($4_{14}-4_{04}$)	18.38	18	101.88	77
$4_{13}-4_{04}$	3100.71282	22 872.615−($4_{14}-4_{04}$)	20.87	22	68.55	73

TABLE 4: Torsional Characterization of Quantum States in the Energy Regions of the cis and gauche Asymmetric Ethylenic Hydride Stretches

energy region (cm^{-1})	N_{cis}	N_{gauche}	$N_{delocalized}$	N_{total}
3060−3160	722	1012	280	2014
3360−3460	1163	1692	498	3353

In principle, the value of the observed state density can provide information about the extent of IVR between states of different conformers.[40] For the cis spectrum, there are large fluctuations in the observed state densities, as seen in Table 1. This may be expected because the weak couplings that characterize this spectrum permit the observation of only the nearest vibrational states. We note that the state densities found for the cis spectrum are much higher than predicted, even if states of all three types of states (cis, gauche, and delocalized) are considered. However, this just reflects the fact that we only sample the smaller level spacings. For the gauche spectrum, the IVR width covers a larger energy region so that the statistics are expected to be more representative of the actual level density. In Figure 8 we show the full state density observed for both of the overlapping gauche spectra. Also shown in Figure 8 are predictions for the state density if only gauche-like states are coupled, if gauche and delocalized are coupled, and if all states (cis, gauche, and delocalized) states are coupled. A $(2J + 1)$ growth of the state density is assumed. This figure illustrates the difficulties associated with this type of analysis. The differences between these cases are less than the spread of observed measurements. Furthermore, our lack of knowledge about the anharmonic corrections to the calculated state density and the effects of limited signal-to-noise ratios in the data make any conclusions tenuous.[46] However, the lack of agreement between the observed state density and the expected state density if all states (cis, gauche, and delocalized) were involved in the vibrational coupling, suggests that the full state density is not available and that, possibly, the cis-like states remain uncoupled from the gauche states.

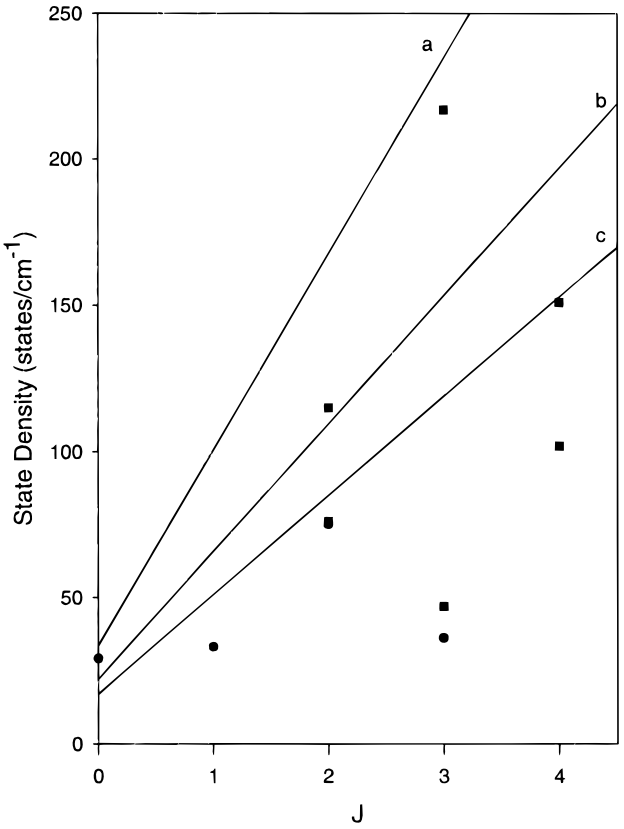

Figure 8. Given here is the state density of both of the overlapping gauche spectra as a function of total angular momentum. The state density is calculated from the central 10 or 20 transition lines of the multiplet, as described in the text. The lines on the figure represent a $(2J + 1)$-growth in the state density calculated when considering (a) all states (cis, gauche and delocalized), (b) only gauche and delocalized states, and (c) only gauche states. The poor agreement between the observed state density and that expected if all states are coupled (line a), suggests that the full density of states is not available and that, possibly, the cis states are not involved in the vibrational coupling to gauche states.

Weak Vibrational Interactions and the Rate of Isomerization. We attribute the slow IVR, or equivalently the weak vibrational coupling, in the cis conformer to the fact that the density of the more strongly coupled cis-like vibrational states are too sparse for extensive coupling. Because the rotational constants of the vibrationally excited cis states are expected to have rotational constants that are close to the bright-state values, the absence of this type of interactions will persist at all values of the rotational quantum numbers. Therefore, the observed coupling is assumed to only reflect the weaker vibrational interactions. The slow IVR rates measured for the cis bright states are similar to the rate of isomerization we have measured in 2-fluoroethanol[16] (2 ns^{-1}) and to weaker "Coriolis" dynamics we have observed in the O−H stretch of propynol[38] (1 ns^{-1}). The Coriolis coupling includes the interaction between rovibrational states with different K_a values, which is known to occur from the observation of a $(2J + 1)$ increase in the measured state density. From the single-photon infrared spectrum it is impossible to determine the actual origin (isomerization vs Coriolis) of these weak interactions

We have examined the matrix element distribution for the weak interactions found in the cis spectrum by performing a Lawrance−Knight deconvolution[47,48] of the spectrum. This analysis provides effective interaction matrix elements between the bright-state and a set of "prediagonalized" bath states. This distribution is shown in Figure 9 and is approximately Gaussian with a mean of zero and width of 106 MHz. We have also examined the J- and K_a-dependence of these matrix elements as shown in Figure 10. Overall, we observe no increase with the total angular momentum J. Also, the distribution is roughly independent of K_a and, if anything, decreases with increasing values of this near quantum number. This result suggests that rovibrational interactions between quantum states of different K_a values are not direct Coriolis interactions which should scale with J (for perpendicular Coriolis interactions) or with K_a (for

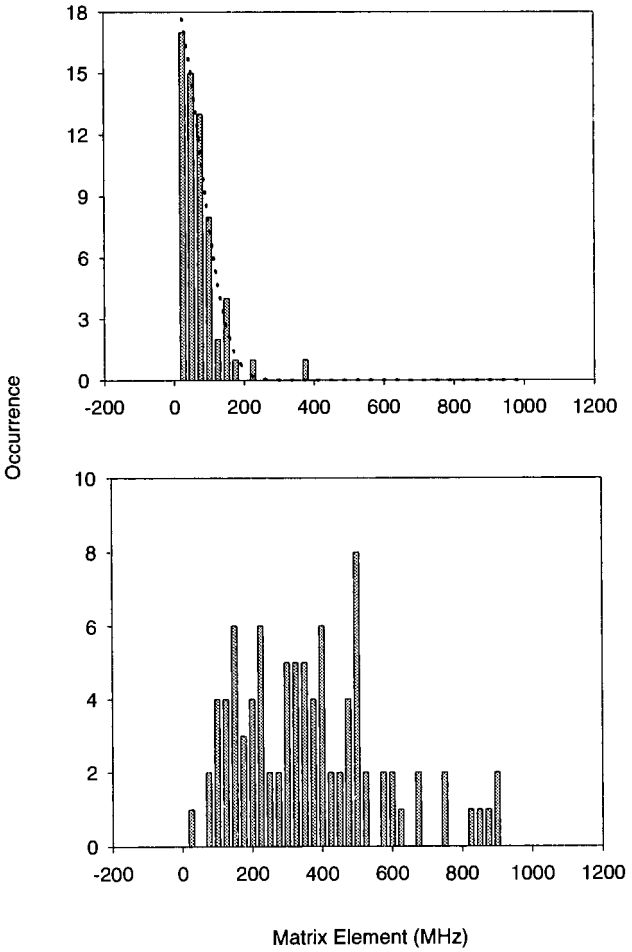

Figure 9. The distribution of the matrix elements that describe the interaction of the bright state to the "prediagonalized" bath states is given for the cis (top) and gauche (bottom) vibrational bands. From the analysis of the cis multiplets, we see that the distribution is Gaussian with zero mean and a width of 106 MHz (σ = 4.7 MHz). The distribution of the gauche matrix elements (here only from the separated 3_{12} and 4_{13} multiplets) shows different behavior. Here, there is an increase in the number of "large" matrix elements that give rise to the faster IVR observed in the gauche vibrational band.

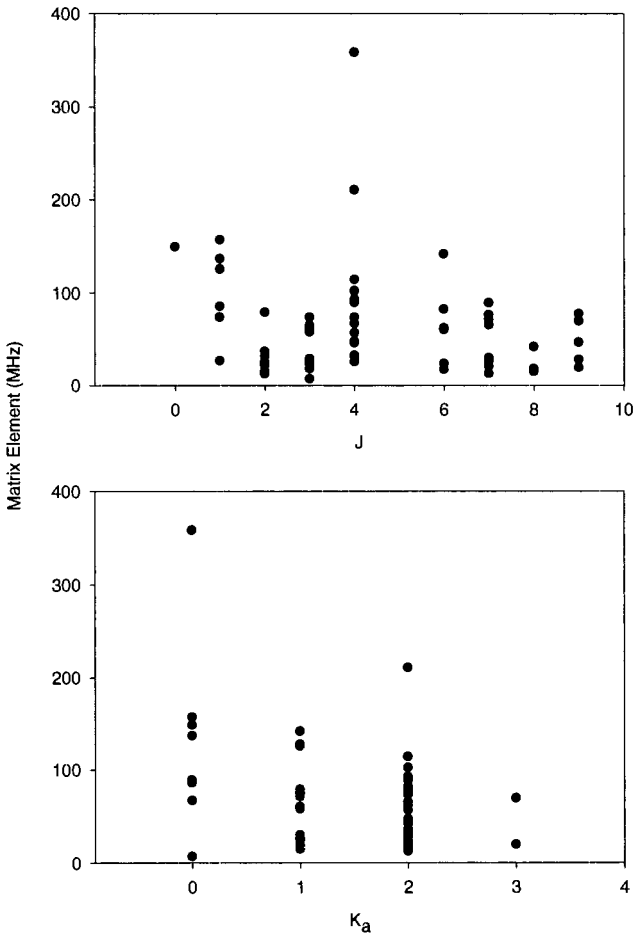

Figure 10. The interaction matrix elements of the cis vibrational band are examined as a function of J (top) and K_a (bottom). As seen in the top panel, the matrix elements are independent of the total angular momentum. The bottom panel shows that the matrix elements are largely independent of K_a as well. As discussed in the text, this indicates that the interactions between quantum states of different K_a values are not direct Coriolis interactions.

parallel Coriolis interactions).[49] This result is consistent with previous IVR studies where a strong increase in the state density is observed with increasing total angular momentum, but there is no corresponding increase in the initial IVR rate.[50] For example, in the acetylenic C−H stretch of propynol, the IVR rate remains nearly constant from $J = 0$ to $J = 9$.[38] The origin of these rovibrational couplings may lie in the nonorthogonality of the rotational wave functions[51] of the different vibrational states as described by Li, Ezra, and Philips, for example.[52]

We have also analyzed the matrix element distribution for the gauche conformer spectrum. To use the Lawrance-Knight deconvolution, the spectra from the two nearly degenerate torsional ground states must first be separated. We have been able to assign the separate spectra for the $3_{12}-3_{03}$ and $4_{13}-4_{04}$ IVR multiplets of the gauche spectrum using ground-state microwave-infrared double-resonance techniques.[24] The matrix element distribution is also shown in Figure 9. One clear difference between the cis and gauche distributions is an increase in the number of "large" matrix elements that give rise to the fast IVR. There is also an indication of a bimodal matrix element distribution composed of a set of weak matrix elements, of magnitude similar to those of the cis spectrum, and the larger values that are typically found in IVR studies of polyatomic molecules of this size.[2]

It is interesting to note that the origin of the large density of near-resonant gauche-like states, compared to the sparse set of cis-like states found near the cis bright state, is the lower torsional frequency of the gauche conformer (108 cm^{-1} for the gauche $v = 0-v = 1$ energy difference vs 164 cm^{-1} for the cis).[29,30] If just the normal-mode frequencies are considered, neglecting the torsional motion, then cis and gauche near-resonant state densities are essentially identical. This comparison implies that the torsionally excited states that remain localized in the gauche well are strongly coupled to the bright state. However, from the cis spectrum, we find that the coupling between cis-like and delocalized (or gauche-like) states is weaker by approximately a factor of 5. This type of level structure leads to IVR dynamics with two separate time scales: a fast vibrational energy redistribution that retains the conformational structure followed by isomerization on a slower time scale, as observed in 2-fluoroethanol.[16,17]

Although the infrared spectrum does not provide direct information about the conformational isomerization rate, it does allow us to calculate the upper limit to the rate following coherent excitation of the asymmetric $=CH_2$ stretch bright state.[17] From the infrared spectrum we can calculate the survival probability.[35] This quantity provides the time scale for energy

TABLE 5: RRKM Parameters and Results for the Unimolecular Isomerization Calculated for cis and gauche Allyl Fluoride in the Asymmetric Ethylenic Hydride Stretch Regions

cis→gauche ($E^*_{cis} \sim 3110$ cm^{-1})		$E_{critical} =$ 1120 cm^{-1}		$E^*_{cis} - E_{critical} \sim$ 1990 cm^{-1}	
ρ_{total}	ρ_{cis}	σ	$N^‡$	τ_{RRKM}	τ_{IVR}
20	7.2	2	121	1 ps	~2000 ps
guache→cis ($E^*_{gau} \sim 3404$ cm^{-1})		$E_{critical} =$ 813 cm^{-1}		$E^*_{gau} - E_{critical}{}^a \sim$ 2300 cm^{-1}	
ρ_{total}	ρ_{gauche}	σ	$N^‡$	τ_{RRKM}	τ_{IVR}
34	16.9	2	222	1.3 ps	~90 ps

[a] ΔE(gauche−cis) = 304 cm^{-1}; therefore, the ρ and $N^‡$ data here is for the 3404 cm^{-1} energy region (all values relative to the cis ZPE) but the $E_{gau}^* - E_{critical}$ value reflects an $E_{gau}^* \sim 3100$ cm^{-1} (relative to the gauche ZPE).

leaving an initial state that has both localized motion (=CH_2 stretch) and conformational structure (cis or gauche). The isomerization rate cannot be faster than the decay rate of the survival probability. For the cis conformer, the typical time scale is 2 ns and for the gauche conformer it is 90 ps. These time scales can be compared to the rates for isomerization predicted by RRKM theory.[4] Because the torsional motion does not change the normal-mode vibrational frequencies very much[30] and because the torsional potential is well characterized experimentally, we believe that all necessary quantities are well determined for this calculation. The RRKM rates, and associated quantities for the rate calculation, are given in Table 5. Theses calculated rates are two to three orders-of-magnitude too fast. This observation is general for molecules of this size where the RRKM isomerization rates are typically 1 ps^{-1}, but the measured survival probability decay times are 40 ps−2 ns.[2,10] Unimolecular isomerization about low barriers appears to be a general class of reactions that are poorly described by RRKM theory.[19−21]

Conclusions

We have observed strongly conformer specific IVR dynamics in the asymmetric =CH_2 stretch spectrum of allyl fluoride. We attribute the differences in the spectra of the cis and gauche conformers to the fact that the vibrational density of states with the same conformation as the bright state place these two spectra in opposite limits. The density of cis states is below the threshold for extensive IVR.[44,45] As a result, we only sample the weaker coupling to states of either delocalized or gauche torsional character and to cis states with different rotational quantum numbers ($\Delta K_a \neq 0$). These weaker rovibrational interactions lead to slow IVR on a 2 ns time scale. Due to the lower torsional frequency of the gauche conformer, there is sufficient state density to observe extensive IVR in this spectrum. The measured IVR lifetime, 90 ps, is similar to that observed in the asymmetric =CH_2 stretch of isobutene[37] (105 ps) and is similar to the IVR rates of other hydride stretches.[2,10]

The implicit assumption in this analysis is that the coupling between vibrational states with the same torsional character (cis or gauche) is stronger than the interactions between vibrational states with different torsional character. The bimodal matrix element distribution resulting from this assumption implies that there are two separate time scales in the dynamics: fast IVR with retention of conformation and slower unimolecular isomerization.[17] Definitive statements about the nature of the coupled states and the strength of the rovibrational coupling are difficult to make from the single-photon infrared spectrum alone. For example, previous work on propynol[38] and 2-fluoroethanol[16] show that the weaker interactions are consistent with both "Coriolis" and cross-conformer coupling strengths. In the following paper we use microwave spectroscopy of the eigenstates of these spectra to show that the conclusions presented here are justified.[22]

Acknowledgment. This work has been supported by the National Science Foundation through CAREER Award CHE-9624850. David A. McWhorter acknowledges support from the Presidential Fellowship program at the University of Virginia.

References and Notes

(1) Baer, T.; Hase, W. L. *Unimolecular Reaction Dynamics, Theory and Experiment*; Oxford University Press: New York, 1996.
(2) Lehmann, K. K.; Scoles, G.; Pate, B. H. *Annu. Rev. Phys. Chem.* **1994**, *45*, 241.
(3) Nesbitt, D. J.; Field, R. W. *J. Phys. Chem.* **1996**, *100*, 12735.
(4) Robinson, P. J.; Holbrook, K. A. *Unimolecular Reactions*; Wiley-Interscience: New York, 1972.
(5) Kommandeur, J.; Majewski, W. A.; Meerts, W. L.; Pratt, D. W. *Annu. Rev. Phys. Chem.* **1987**, *38*, 443.
(6) Leinau, C.; Heikal, A. A.; Zewail, A. H. *Chem. Phys.* **1993**, *175*, 171.
(7) Hamm, P.; Lim, M.; Hochstrasser, R. M. *J. Chem. Phys.* **1997**, *107*, 10523.
(8) Arrivo, S. M.; Heilweil, E. J. *J. Phys. Chem.* **1996**, *100*, 11975.
(9) Quack, M.; Stoher, J. *J. Phys. Chem.* **1993**, *97*, 12574.
(10) Bethardy, G. A.; Wang, X.; Perry, D. S. *Can. J. Chem.* **1994**, *72*, 652.
(11) Perry, D. S.; Bethardy, G. A.; Wang, X. *Ber. Bunsen-Ges. Phys. Chem.* **1995**, *99*, 530.
(12) Ruoff, R. S.; Klots, T. D.; Emilsson, T.; Gutowsky, H. S. *J. Chem. Phys.* **1990**, *93*, 3142.
(13) McIlroy, A.; Nesbitt, D. J. *J. Chem. Phys.* **1990**, *92*, 2229.
(14) Hudspeth, E.; McWhorter, D. A.; Pate, B. H. *J. Chem. Phys.* **1997**, *107*, 8189.
(15) Green, D.; Hammond, S.; Keske, J.; Pate, B. H. *J. Chem. Phys.* Submitted for publication.
(16) McWhorter, D. A.; Hudspeth, E.; Pate, B. H. *J. Chem. Phys.* Submitted for publication.
(17) Pate, B. H. *J. Chem. Phys.* Submitted for publication.
(18) a) Kato, T. *J. Chem. Phys.* **1998**, *108*, 6611. (b) Steinfeld, J. I.; Francisco, J. S.; Hase, W. L. *Chemical Kinetics and Dynamics*; Prentice-Hall: NJ; 1989.
(19) Nordholm. S. *J. Chem. Phys.* **1989**, *137*, 109.
(20) Northrup. S. H.; Hynes, J. T. *J. Chem. Phys.* **1980**, *73*, 2700.
(21) Leitner, D. M.; Wolynes, P. G. *Chem. Phys. Lett.* **1997**, *280*, 411.
(22) McWhorter, D. A.; Pate, B. H. *J. Phys. Chem. A* **1998**, *102*, 8795.
(23) Lee, C. Y.; Pate, B. H. *Chem. Phys. Lett.* **1997**, *284*, 369.
(24) Lee, C. Y.; Pate, B. H. *J. Chem. Phys.* **1997**, *107*, 10430.
(25) Fraser, G. T.; Pine, A. S. *J. Chem. Phys.* **1989**, *91*, 637.
(26) Hirota, E. *J. Chem. Phys.* **1965**, *42*, 2071.
(27) McLachlan, R. D.; Nyquist, R. A. *Spectrochim. Acta* **1968**, *24*, 103.
(28) Meakin, P.; Harris, D. O.; Hirota, E. *J. Chem. Phys.* **1969**, *51*, 3775.
(29) Durig, J. R.; Zhen, M.; Little, T. S. *J. Chem. Phys.* **1984**, *81*, 4259.
(30) Durig, J. R.; Geyer, T. J.; Little, T. S.; Durig D. T. *J. Mol. Struct.* **1988**, *172*, 165.
(31) Luppi, J.; Rasanen, M.; Murto, J.; Pajunen, P. *J. Mol. Struct.* **1991**, *245*, 307.
(32) The current discussion of relative and absolute energies, as well as the state counting calculations, relies on the experimental torsional potential reported in ref 29.
(33) Bowman, J. M.; Gazdy, B. *J. Phys. Chem. A.* **1997**, *101*, 6384.
(34) For a full list of eigenstate positions and intensities, see: McWhorter, D. A. Ph.D. thesis, University of Virginia, August 1998.
(35) Jiang. X.; Brumer, P. *J. Chem. Phys.* **1991**, *94*, 5833.
(36) Bethardy, G. A.; Perry, D. S. *J. Chem. Phys.* **1993**, *98*, 6651.
(37) McWhorter, D. A.; Pate, B. H. *J. Mol. Spectrosc.* Submitted for publication.
(38) Hudspeth, E.; McWhorter, D. A.; Pate, B. H. *J. Chem. Phys.* **1998**, *109*, 4316.
(39) Boyarkin, O. V.; Lubich, L.; Settle, R. D. F.; Perry, D. S.; Rizzo, T. R. *J. Chem.* Phys. To be submitted for publication.
(40) Cupp, S.; Lee, C. Y.; McWhorter, D. A.; Pate B. H. *J. Chem. Phys.* **1998**, *109*, 4302.
(41) Kemper, M. J. H.; van Dijk, J. M. F.; Buck H. M. *Chem. Phys. Lett.* **1978**, *53*, 121.

(42) Lewis, J. D.; Mallory, T. B.; Chao, T. H.; Laane, J. *J. Mol. Struct*. **1972**, *12*, 427.

(43) Andrews, A. M.; Fraser, G. T.; Pate, B. H. *J. Chem. Phys*. **1998**, *109*, 4290.

(44) Kim, H. L.; Kulp, T. J.; McDonald, J. D. *J. Chem. Phys*. **1987**, *87*, 4376.

(45) Pate, B. H.; Lehmann, K. K.; Scoles, G. *J. Chem. Phys*. **1991**, *95*, 3891.

(46) Extensive numerical modeling of these effects have been presented in: Perry, D. S. *J. Chem. Phys*. **1993**, *98*, 6665.

(47) Lawrance, W. D.; Knight, A. E. W. *J. Phys. Chem.* **1985**, *89*, 917.

(48) Lehmann, K. K. *J. Phys. Chem.* **1991**, *95*, 7556.

(49) Papousek, D.; Aliev, M. R. *Molecular Vibrational Rotational-Spectra. Theory and Applications of High-Resolution Infrared, Microwave and Raman Spectroscopy of Polyatomic Molecules*; Elsevier: Amsterdam, Netherlands, 1981.

(50) For examples of this effect, see refs 37 and 38.

(51) Miller, C. C.; Philips, L. A.; Andrews, A. M.; Fraser, G. T.; Pate, B. H.; Suenram, R. D. *J. Chem. Phys*. **1994**, *100*, 831.

(52) Li, H.; Ezra, G. S.; Philips, L. A. *J. Chem. Phys*. **1992**, *97*, 5956.